Molecular Biology of the Cell
Vol. 12, 711–723, March 2001

A Family of Small Coiled-Coil–forming Proteins Functioning at the Late Endosome in Yeast

Andreas Kranz, Andrea Kinner, and Ralf Kölling*

Institut für Mikrobiologie, Heinrich-Heine-Universität Düsseldorf, D-40225 Düsseldorf, Germany

Submitted March 20, 2000; Revised November 20, 2000; Accepted January 9, 2000
Monitoring Editor: Hugh R.B. Pelham

The multispanning membrane protein Ste6, a member of the ABC-transporter family, is transported to the yeast vacuole for degradation. To identify functions involved in the intracellular trafficking of polytopic membrane proteins, we looked for functions that block Ste6 transport to the vacuole upon overproduction. In our screen, we identified several known vacuolar protein sorting (*VPS*) genes (*SNF7/VPS32*, *VPS4*, and *VPS35*) and a previously uncharacterized open reading frame, which we named *MOS10* (more of Ste6). Sequence analysis showed that Mos10 is a member of a small family of coiled-coil–forming proteins, which includes Snf7 and Vps20. Deletion mutants of all three genes stabilize Ste6 and show a "class E *vps* phenotype." Maturation of the vacuolar hydrolase carboxypeptidase Y was affected in the mutants and the endocytic tracer FM4-64 and Ste6 accumulated in a dot or ring-like structure next to the vacuole. Differential centrifugation experiments demonstrated that about half of the hydrophilic proteins Mos10 and Vps20 was membrane associated. The intracellular distribution was further analyzed for Mos10. On sucrose gradients, membrane-associated Mos10 cofractionated with the endosomal t-SNARE Pep12, pointing to an endosomal localization of Mos10. The growth phenotypes of the mutants suggest that the "Snf7-family" members are involved in a cargo-specific event.

INTRODUCTION

The exocytic/endocytic membrane system of the eukaryotic cell consists of numerous membrane-bound organelles that continuously exchange material with each other by transport intermediates. There is evidence that this complex and highly dynamic array of membrane compartments may be a self-organizing system that can be disassembled and rebuilt. This has been documented for the Golgi apparatus, which is broken down during mitosis and reassembled during interphase (Zaal *et al.*, 1999). It is still unclear what determines the identity of the different compartments in this highly dynamic system and how this identity is maintained despite continuous exchange.

In yeast, a large number of gene functions involved in protein trafficking have been identified through genetic screens (Jones, 1977; Novick *et al.*, 1980; Bankaitis *et al.*, 1986; Rothman and Stevens, 1986; Robinson *et al.*, 1988; Weisman *et al.*, 1990; Wada *et al.*, 1992). To identify additional functions important for protein trafficking, we looked for functions that block protein transport upon overproduction. As a model protein for the investigation of protein trafficking, we used the **a**-factor transporter Ste6, like cystic fibrosis transmembrane conductance regulator and multidrug resistance proteins, a member of the ABC-transporter family (Kuchler *et al.*, 1989; McGrath and Varshavsky, 1989). Ste6 is an integral membrane protein with two homologous ABC-transporter motifs each consisting of six transmembrane spanning segments and a conserved ATP-binding domain. The two halves of Ste6 are connected by a linker region, which we have shown to be important for the regulation of Ste6 turnover (Kölling and Losko, 1997). Ste6 starts its itinerary through the cell at the endoplasmic reticulum from where it is transported to the cell surface. It stays there only transiently, due to efficient endocytosis. We have presented evidence that ubiquitination of Ste6 is important for determining the residence time at the cell surface (Kölling and Hollenberg, 1994). Following endocytosis, Ste6 is transported to the vacuole where it is degraded. Ste6 is a very short-lived protein with a half-life of ~20 min. Its degradation is strongly affected by mutations in vacuolar hydrolase genes but is unaffected by mutations in proteasomal subunits (Kölling and Losko, 1997).

Here, we report the isolation of functions that block transport of Ste6 to the vacuole upon overproduction. The transport block is reflected in a stabilization of the protein. In addition to already described vacuolar protein sorting (*vps*) functions, like *SNF7/VPS32*, *VPS4* (Babst *et al.*, 1998), and *VPS35* (Seaman *et al.*, 1998), we identified a previously uncharacterized gene function that we named *MOS10* (more of Ste6). Sequence comparisons showed that Mos10 forms a family of small coiled-coil–forming proteins together with Snf7 and Vps20. Although all three family members appear

* Corresponding author. E-mail address: ralf.koelling@uni-duesseldorf.de.

Table 1. Yeast strains

Strain	Genotype	Reference
JD52	*MAT**a** ura3-52 his3-Δ200 leu2-3,112 trp1-Δ63 lys2-801*	J. Dohmen
RKY901	*MAT**a** ura3-52 his3-Δ200 leu2-3,112 trp1-Δ63 lys2-801 ste6::(STE6-lacZ CYC1$_{term}$ TRP1)*	This study
RKY1452	*MAT**a** ura3-52 his3-Δ200 leu2-3,112 trp1-Δ63 lys2-801 MOS10-13myc::kan′*	This study
RKY1509	*MAT**a** ura3-52 his3-Δ200 leu2-3,112 trp1-Δ63 lys2-801 Δmos1::kan′*	This study
RKY1510	*MAT**a** ura3-52 his3-Δ200 leu2-3,112 trp1-Δ63 lys2-801 Δsnf7::HIS3*	This study
RKY1511	*MAT**a** ura3-52 his3-Δ200 leu2-3,112 trp1-Δ63 lys2-801 Δvps4::HIS3*	This study
RKY1517	*MAT**a** ura3-52 his3-Δ200 leu2-3,112 trp1-Δ63 lys2-801 MOS10-13myc::kan′ Δvps4::HIS3*	This study
RKY1590	*MAT**a** ura3-52 his3-Δ200 leu2-3,112 trp1-Δ63 lys2-801 Δvps20::HIS3*	This study
RKY1633	*MAT**a** ura3-52 his3-Δ200 leu2-3,112 trp1-Δ63 lys2-801VPS20-13myc::HIS3*	This study

to be involved in the same trafficking step, i.e., endosome-to-vacuole transport, they show different growth phenotypes. This suggests that they are involved in a cargo-specific event.

MATERIALS AND METHODS

Plasmids

All multicopy plasmids with *VPS* genes are based on the vector YEplac181 (Gietz and Sugino, 1988). The plasmid pRK567 contains a 1.8-kb *Hin*dIII chromosomal *VPS4* fragment from a *Saccharomyces cerevisiae* gene bank plasmid. The other *VPS* genes were generated by polymerase chain reaction (PCR) from chromosomal template DNA. For cloning, unique restriction sites flanking the corresponding genes were introduced by PCR. Plasmid pRK585 contained *SNF7* on a 1.8-kb *Eco*RI/*Hin*dIII fragment, pRK586 *VPS35* on a 3.8-kb *Eco*RI/*Pst*I fragment, and pRK587 *MOS10* on a 1.4-kb *Eco*RI/*Pst*I fragment. To construct the *STE6-GFP* plasmid pRK599, a new *Sal*I site was introduced into the *STE6* gene by PCR just upstream of the stop codon. A 4.5-kb *Bgl*II-*Sal*I fragment of this modified *STE6* gene and a 740-bp *Xho*I/*Sal*I PCR-fragment, encoding an S65G/S72A GFP variant were cloned into the vector YEplac195 (Gietz and Sugino, 1988) upstream of a *CYC1* terminator fragment.

Yeast Strains

Yeast strains are listed in Table 1. All strains are directly derived from JD52. To generate RKY901, a cassette containing the *TRP1* selection marker, a C-terminal *STE6*-fragment fused to lacZ and a *CYC1* terminator fragment was integrated into the chromosomal *STE6* locus by homologous recombination, resulting in a complete copy of *STE6* fused to *lacZ* and a defective *STE6* copy truncated at the N terminus. The strains RKY1452, RKY1509, RKY1510, RKY1511, RKY1517, RKY1590, and RKY1633 were generated by PCR-based gene deletion or modification as described (Longtine *et al.*, 1998). All gene modifications were verified by at least two independent, specific PCR reactions.

Immunofluorescence and Green Fluorescent Protein (GFP) Staining

The immunofluorescence experiments were performed as described previously (Kölling and Hollenberg, 1994). Ste6-c-myc was detected with the anti-c-myc primary antibody 9E10 (1:200; Berkeley Antibody, Richmond, CA) and with fluorescein isothiocyanate (FITC)-conjugated anti-mouse secondary antibodies (1:300; Dianova, Hamburg, Germany). To examine GFP fluorescence (Tsien, 1998), cells were grown overnight to exponential phase (A_{600} = 0.5–0.8, 3–4 × 10^7 cells/ml) in minimal medium (YNB; Difco, Detroit, MI) supplemented with required nutrients. Cells were fixed on a microscope slide by mixing with low melting agarose. Fluorescence was visualized with a Zeiss Axioskop microscope using an FITC filter set. Images were acquired with a charge-coupled device camera (Sony, Tokyo, Japan).

FM4-64 Internalization

Cells were grown overnight to exponential phase (A_{600} = 0.5–0.8, 3–4 × 10^7 cells/ml) in rich medium (YPD). Cells (500 μl, 2 × 10^7 cells) were pelleted at 400 × *g* for 1 min and resuspended in 100 μl of fresh medium. FM4-64 (Molecular Probes, Eugen, OR) was added to 40 μM from a stock solution of 16 mM in dimethyl sulfoxide, followed by an incubation with shaking at 30°C. After 15 min, the cells were washed with fresh medium and chased for 45–60 min. For observation, cells were fixed on a microscope slide by mixing with low melting agarose. The FM4-64 fluorescence was observed with a Rhodamine filter set.

LacZ Filter Tests

Freshly grown colonies (2–3 d old) were transferred to nitrocellulose or nylon membranes. The membranes were submerged in liquid nitrogen for 10 s to break the cells and then placed on filter paper soaked with 1.5 ml of Z-buffer (0.1 M Na_2PO_4, 10 mM KCl, 1 mM $MgSO_4$) containing 15 μl of a X-Gal stock solution (100 mg/ml in dimethyl sulfoxide). The membranes were incubated at 30°C until the indigo blue color was clearly visible. All reactions were stopped simultaneously by removing the membranes from the filter paper.

Differential Centrifugation

Four A_{600} units of cells from an exponentially growing culture (A_{600} = 0.4–0.7, 2–4 × 10^7 cells/ml) were harvested, washed in H_2O, resuspended in lysis buffer (0.3 M sorbitol, 50 mM HEPES pH 7,5, 10 mM NaN_3), and lysed by vortexing with glass beads for 3 min. Intact cells and cell debris were removed by centrifugation at 500 × *g* for 5 min. To test for detergent solubility, the samples were incubated on ice for 30 min with 2% Triton X-100 before centrifugation. The cell extract was centrifuged at 13,000 × *g* for 10 min to pellet the P13 fraction. The supernatant was spun again at 100,000 × *g* for 1 h to generate the P100 pellet and the S100 supernatant. Equal portions of the fractions were assayed for the presence of proteins by Western blotting.

Carboxypeptidase Y (CPY) Sorting

Cells were grown to exponential phase (A_{600} = 0.4–0.7) in minimal medium supplemented with required nutrients. Cells (0.5 A_{600} units) resupended in 0.5 ml of the same medium with 1 mg/ml IgG-free bovine serum albumin (Sigma, St. Louis, MO) were labeled for 10 min with 100 μCi [^{35}S] Trans label (Amersham, Freiburg, Germany) and chased with an excess of cold methionine and cysteine for another 40 min at 30°C. After the addition of 0.5 ml of 2×

S-Buffer (2.4 M sorbitol, 1 M Tris/HCl pH 7.5, 20 mM NaN_3, 2 mM $MgCl_2$, 40 μM dithiothreitol, and protease inhibitors) and a 5-min incubation on ice, the cells were spheroplasted by the addition of 20 μg of zymolyase for 25 min at 30°C. Spheroplasts were centrifuged for 2 min at 700 × *g* and resuspended in sample buffer to form the internal fraction. The proteins contained in the supernatant were trichloroacetic acid-precipitated and resuspended in sample buffer to form the external fraction. Immunoprecipitation was performed as described previously. The precipitated proteins were analyzed by SDS-PAGE and autoradiography.

Other Methods

Pulse chase experiments, immunoprecipitation, and cell fractionation by sucrose density gradients were essentially performed as described previously (Kölling and Hollenberg, 1994) except that the cells for the sucrose density gradients were harvested by vacuum filtration onto nitrocellulose filters and not by centrifugation. Following filtration, the cells were immediately resuspended in STED10 buffer (10% sucrose, 10 mM Tris/HCl pH 7.6, 10 mM EDTA, 1 mM dithiothreitol) and lysed by vortexing with glass beads for 3 min.

RESULTS

Identification of Gene Functions That Stabilize Ste6 upon Overproduction

To identify gene functions involved in Ste6 trafficking to the vacuole, we looked for genes that stabilize Ste6 upon overproduction. A block in transport to the vacuole should lead to a prolonged half-life of Ste6, which in turn should result in a higher steady-state level of the protein. Because the amount of Ste6 in the cell cannot be easily quantified based on its own activity, we fused Ste6 at its C terminus with *Escherichia coli* β-galactosidase (LacZ) whose activity can be easily measured. The Ste6-LacZ fusion was fully functional in a mating assay and like normal Ste6 (Kölling and Hollenberg, 1994) accumulated at the plasma membrane in an endocytosis mutant, indicating that it was properly transported to the cell surface (our unpublished results). Strain RKY901 containing the *STE6-lacZ* cassette integrated into the yeast genome was transformed with a yeast chromosomal DNA library based on the multicopy vector YEp13. The transformants were transferred to nitrocellulose filters and were assayed for LacZ activity by incubation with X-gal, which is converted to a blue dye by β-galactosidase. Among 25,000 greenish-blue transformants 15 colonies with a darker blue color were detected. Plasmids were isolated from these transformants and after retransformation and retesting, the identity of the plasmid inserts was determined by sequencing. The open reading frames responsible for the increased LacZ activity were narrowed down by subcloning. From the five different genes identified, three (*VPS4*, *SNF7/VPS32*, and *VPS35*) had been implicated previously in trafficking of proteins to the yeast vacuole (Babst *et al.*, 1998; Seaman *et al.*, 1998). Another function identified was the *STE5* gene. Because it is known that Ste5 overproduction activates the pheromone response pathway (Akada *et al.*, 1996) and because *STE6* expression is increased by mating pheromone (Erdman *et al.*, 1998), the higher Ste6-LacZ level is probably the result of a higher expression from the *STE6* promoter. For this reason, *STE5* was not characterized any further. In addition to the known genes, a previously uncharacterized open reading frame, *YDR486c*, was identified. We named this gene *MOS10*.

A higher Ste6-LacZ level may result from increased *STE6* expression or from reduced Ste6 turnover. To distinguish between these two alternatives, the Ste6 half-life was determined by pulse-chase experiments in the wild-type strain JD52 transformed with the identified genes on multicopy plasmids. After a 15-min pulse with [^{35}S]methionine, chase was initiated and samples were taken at time intervals and analyzed for the presence of Ste6 by immunoprecipitation, SDS-PAGE, and autoradiography. As reported previously (Kölling and Hollenberg, 1994), a very short half-life (13 min) was observed with the vector control (Figure 1A). Overexpression of *MOS10* (Figure 1B), *SNF7* (Figure 1C), or *VPS4* (Figure 1D), however, stabilized Ste6 approximately two- to fivefold. This shows that the higher Ste6-LacZ level is indeed the result of reduced Ste6 turnover and not the result of increased gene expression. No significant stabilization (τ = 17 min) was observed with *2 μ-VPS35* (Figure 1E). There appeared to exist a strong selective pressure against a high copy number of the 2 μ plasmids. We noticed that the dark blue color in the LacZ filter test disappeared after continued passaging of the RKY901 transformants. Good results were only observed with fresh transformants. The effects of overexpression on Ste6 turnover may thus be lost upon passaging of the cells.

In the following, we focused on the *MOS10*, *SNF7*, and *VPS4* genes. To examine the effects of a loss of these gene functions on Ste6 turnover, deletion mutants were constructed. All deletion mutants turned out to be viable under standard growth conditions (Figure 4A). The Ste6 half-life was determined in the mutants by pulse-chase experiments. As can be seen from Figure 2, Ste6 was stabilized ~10-fold in the Δ*mos10* and Δ*vps4* mutants ($\tau \approx$100 min) and approximately fivefold in the Δ*snf7* mutant (τ = 49 min). These experiments show that not only overproduction but also deletion of these gene functions lead to a stabilization of Ste6.

A New Family of Coiled-Coil–forming Proteins

The *MOS10* gene codes for a 29.7-kDa hydrophilic protein. A "BLAST search" revealed significant sequence similarity to other yeast proteins, to Snf7 that was also isolated in our screen, and to a protein encoded by open reading frame *YMR077c*, which corresponds to the *VPS20* gene (Emr, personal communication). Like Δ*mos10* and Δ*snf7*, the *VPS20* deletion also stabilized Ste6 (Figure 2). The alignment presented in Figure 3B shows that the similarity extends over the whole length of the proteins. About the same degree of identity (30%) was observed between Snf7 and the other two proteins. Similarity between Mos10 and Vps20, however, was barely detectable (15% identity). This suggests that Snf7 is the ancestor of this small protein family and that Mos10 and Vps20 diverged from the Snf7 sequence. A computer program based on the COILS algorithm (Lupas, 1996) predicts that all three proteins contain coiled-coil–forming regions (Figure 3A). In general, this protein motif is involved in protein–protein interactions with other coiled-coil–forming proteins. This indicates that the proteins of the Snf7 family may form a complex either with themselves or with other proteins. Interestingly, the coiled-coil motifs

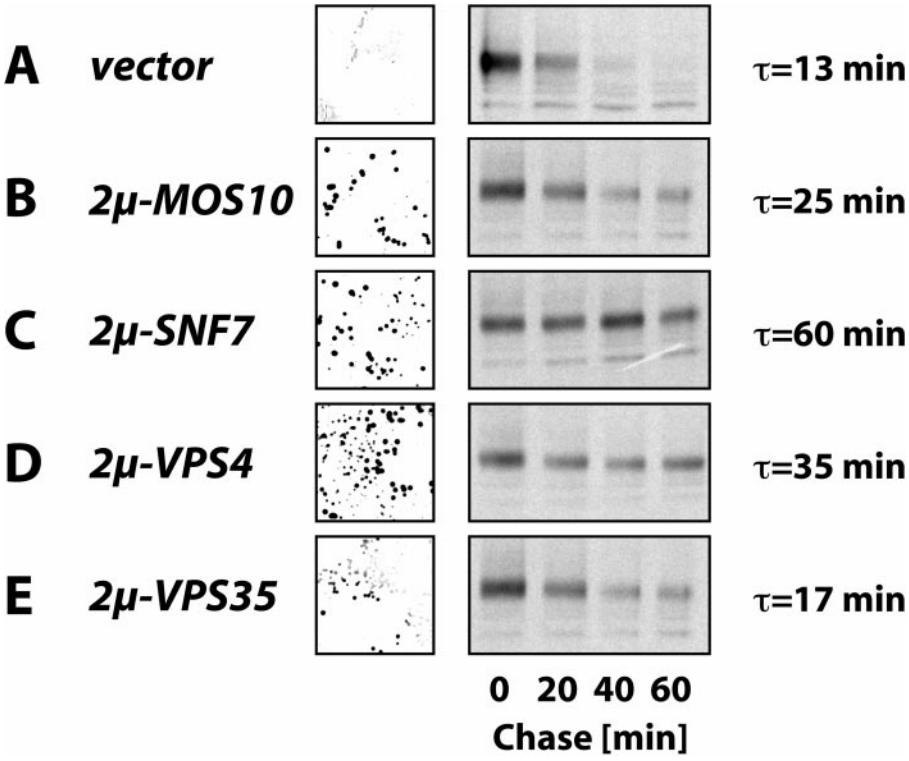

Figure 1. Stabilization of Ste6 through overproduction of gene products. (Left) Strain RKY901, which contains a chromosomal *STE6-lacZ* fusion, was transformed with multicopy plasmids carrying different genes. The transformants were tested for LacZ activity by a filter assay. LacZ activity is reflected in a dark blue color of the colonies. (Right) Ste6 half-life in strain JD52 transformed with the multicopy plasmids was determined by pulse-chase experiments. Cells were labeled with [^{35}S] Trans label for 15 min and were then chased with an excess of cold methionine and cysteine for the time intervals indicated. Ste6 was precipitated from cell extracts with polyclonal antibodies directed against Ste6. The transformed plasmids were YEplac181 (vector control) (A), pRK587 (2μ-MOS10*) (B), pRK585 (*2μ-*SNF7*) (C), pRK567 (*2μ-VPS4*) (D), and pRK586 (*2μ-*VPS35*) (E). The calculated Ste6 half-lives are shown at the right side of the diagram.

are not always found at the same positions in the proteins. This could mean that in each case different parts of the proteins are engaged in interaction with their binding partners.

SNF7 (sucrose nonfermenting) was originally identified as a mutant unable to fully derepress invertase on low-glucose medium and thus unable to grow on media containing raffinose as a carbon source (Tu *et al.*, 1993). In addition, a temperature-sensitivity phenotype has been reported for this mutant. We tested whether *MOS10*, *VPS20*, and *VPS4* deletions had phenotypes similar to Δ*snf7* (Figure 4). Like Δ*snf7*, the Δ*vps20* mutant was temperature sensitive and showed poor growth on media containing raffinose (Figure 4, B and C). The Δ*mos10* mutant, however, grew like wild type at high temperature and on raffinose plates. Thus, despite their similarity, Mos10 and Snf7 appear to perform separate functions. This is also supported by the finding that overproduction of Mos10 is not able to suppress the Δ*snf7* growth phenotypes (our unpublished results). The Δ*vps4* mutant showed an intermediary phenotype; its growth rate

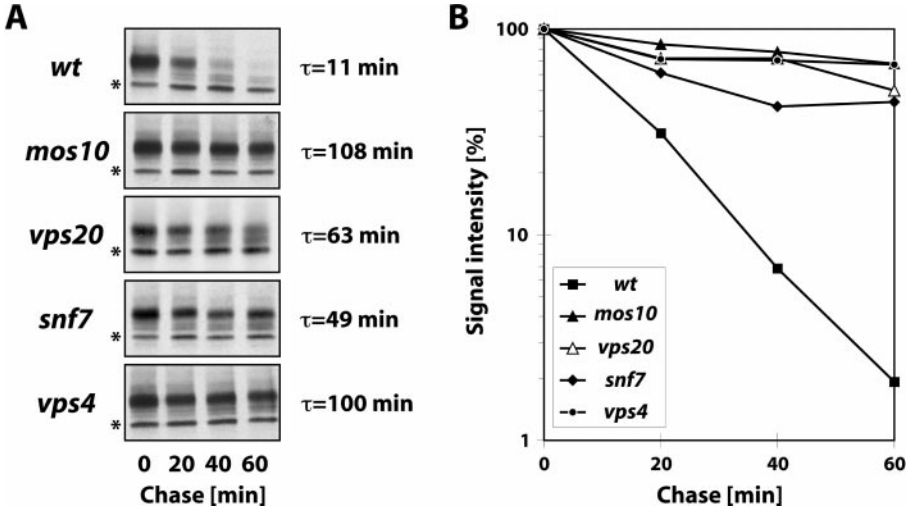

Figure 2. Ste6 stability in deletion mutants. (A) Ste6 half-life was determined in wild-type and in different deletion mutants by pulse-chase experiments. Cells were labeled with [^{35}S] Trans label for 15 min and were then chased with an excess of cold methionine and cysteine for the time intervals indicated. Ste6 was precipitated from cell extracts with polyclonal antibodies directed against Ste6. The strains were (from top to bottom) JD52 (wild-type), RKY1509 (Δ*mos10*), RKY1590 (Δ*vps20*), RKY1510 (Δ*snf7*), and RKY1511 (Δ*vps4*). A background band unrelated to Ste6 is marked by an asterisk. (B) Semilogarithmic plots of the signal intensities quantified by densitometry. The half-lives calculated from the curves in B are shown in A.

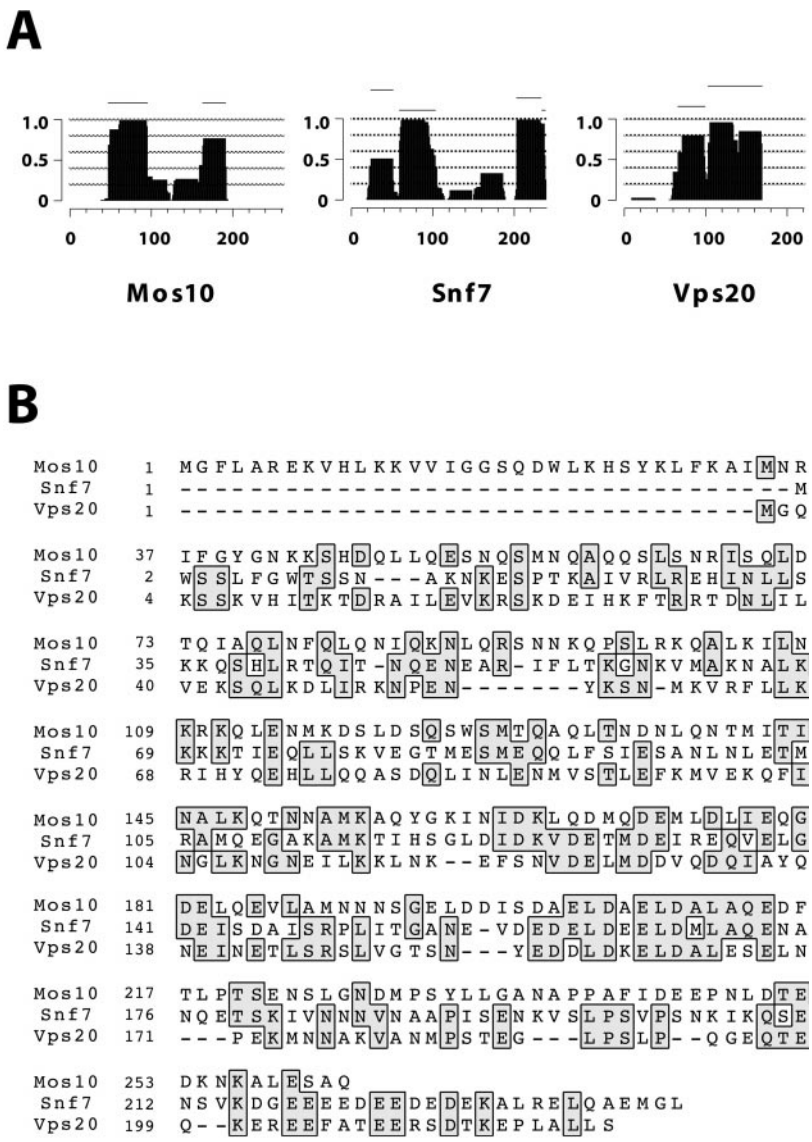

Figure 3. Sequence alignment and coiled-coil forming ability of the Snf7 family members. (A) Mos10 (*YDR486c*), Snf7, and Vps20 (*YMR077c*) were analyzed for coiled-coil–forming regions with the program Macstripe 2.0a1 by Alex Knight, which is based on the COILS algorithm of Andrei Lupas (Lupas, 1996). Displayed is the potential of coiled-coil formation. The bars on top of the diagrams indicate the possible frames of the heptad repeats. (B) Alignment of the proteins generated with ClustalX. Residues identical in two out of three sequences are boxed.

was somewhat reduced at high temperature and on raffinose plates.

CPY-sorting Is Defective in the Δmos10 Mutant

The *snf7*, *vps4*, and *vps20* mutants block endosome-to-vacuole trafficking and accumulate a structure, the so-called "class E compartment", corresponding to the late endosome in yeast (Raymond *et al.*, 1992; Babst *et al.*, 1998). To test whether *mos10* as well has a defect in the vacuolar biogenesis pathway, we examined the processing of the vacuolar protease CPY by pulse-chase experiments. The CPY precursor is characteristically modified along its trafficking pathway to the vacuole. In the endoplasmic reticulum it is core glycosylated to the p1-form, in the Golgi it is converted into the slower migrating, outer-chain glycosylated p2-form, and in the vacuole the mature m-form is finally generated by proteolytic cleavage of the precursor (Figure 5, lanes 1–4). Under normal conditions, CPY is completely converted to the mature form after a 30-min chase period. Internal and external fractions were analyzed for the presence of CPY forms after 10-min labeling with [^{35}S]methionine and a 40-min chase period (Figure 5). With wild type, CPY was exclusively found in its mature form in the internal fraction after 40 min of chase, indicating that CPY was properly delivered to the vacuole. With the Δ*snf7*, Δ*vps4*, and Δ*vps20* mutants, a certain fraction of missorted CPY was found in its Golgi-modified p2-form in the external fraction, as reported previously (Robinson *et al.*, 1988; Babst *et al.*, 1997). Still, most of CPY was in its mature form in the internal fraction. CPY sorting was also affected in the Δ*mos10* mutant. However, the CPY sorting pattern was somewhat different compared with the other mutants. In contrast to the other mutants, a higher amount of internal p1-CPY was observed in the Δ*mos10* mutant. A small

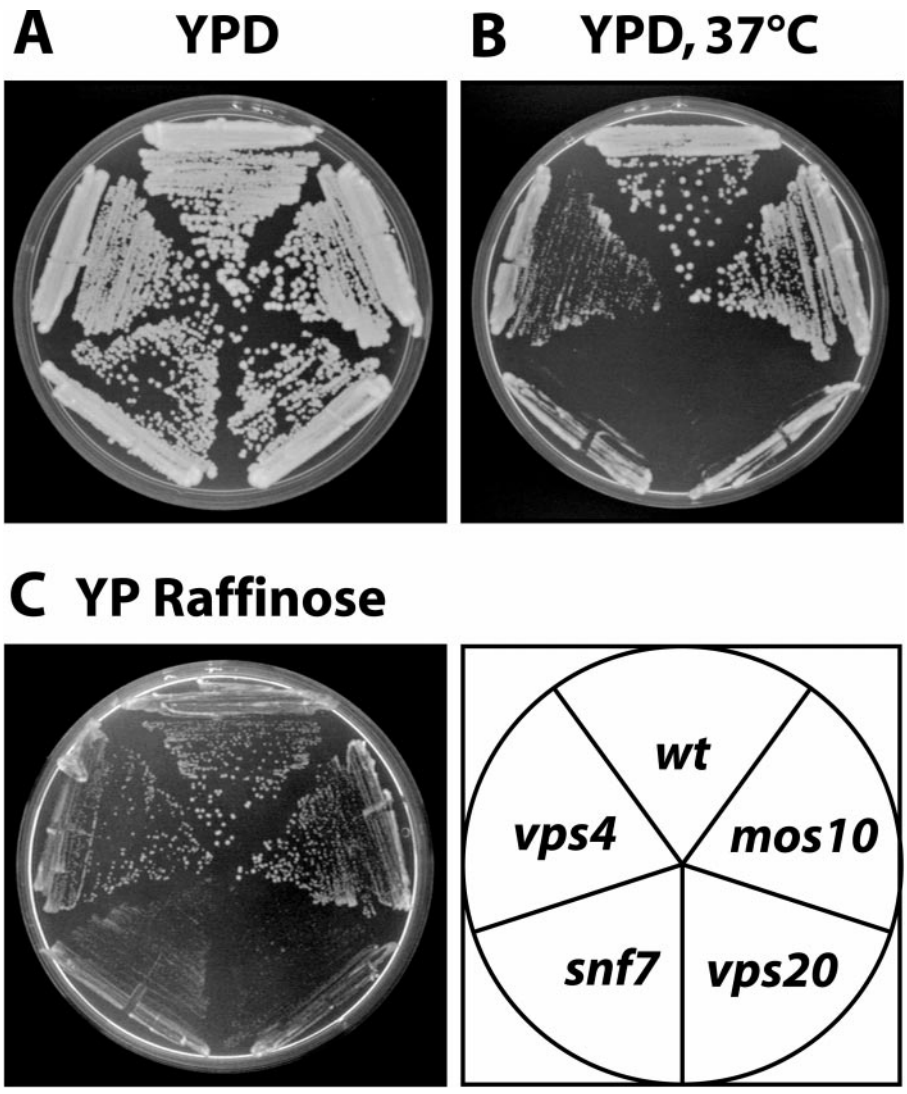

Figure 4. Growth properties of the deletion strains. JD52 (wild-type), RKY1509 (Δ*mos10*), RKY1590 (Δ*vps20*), RKY1510 (Δ*snf7*), RKY1511 (Δ*vps4*) were streaked out on YPD plates (A and B) and on YP-raffinose plates (C). The plates were incubated for 3 d at 30°C (A and C) or at 37°C (B).

amount of p2-CPY was also detected in the external fraction (up to 10% of total CPY). The amount of external p2-CPY in the Δ*mos10* mutant was variable between different experiments (our unpublished results). The reason for this variability in unknown.

For all three Snf7 family mutants, the amount of p2-CPY detected in the external fraction was very low (≈10% of total CPY). To exclude that a substantial fraction of p2-CPY is lost during the experiment, we compared the amount of labeled CPY present at 0-min time point with the amount of labeled CPY after 40 min of chase. After a short 5-min pulse, internal and external fractions were analyzed for the presence of CPY at 0 and 40 min of chase. As can be seen in Figure 6, the total amount of CPY was not significantly reduced during the 40-min chase period. For the strains tested, the fractions recovered after 40 min of chase were wild type = 85%, Δ*mos10* = 95%, and Δ*vps4* = 100%. These experiments show that the low amount of p2-CPY in the external fraction cannot be attributed to a selective loss of p2-CPY during the experiment.

Deletion of MOS10 Causes a "class E" vps *Phenotype*

If endosome-to-vacuole trafficking were affected in Δ*mos10*, transport of endocytic markers to the vacuole should be defective. To test the integrity of the endocytic pathway, transport of the vital stain FM4-64 used to follow bulk membrane internalization and transport to the vacuole (Vida and Emr, 1995) was examined. In the wild-type strain, FM4-64 was rapidly internalized and accumulated specifically in the vacuolar membrane (Figure 7A). The vacuoles can be seen as indentations in the Nomarsky image. Transport to the vacuole was energy-dependent. In cells depleted for ATP by the addition of azide (which blocks respiration), FM4-64 accumulated in small peripheral dots, which presumably correspond to early endosomes (Figure 7B). In Δ*snf7*, Δ*vps4*, and Δ*vps20* with a known block in endosome-to-vacuole trafficking, FM4-64 accumulated asymmetrically at the vacuolar membrane either in form of a crescent-shaped staining on one side of the vacuole or in form of a

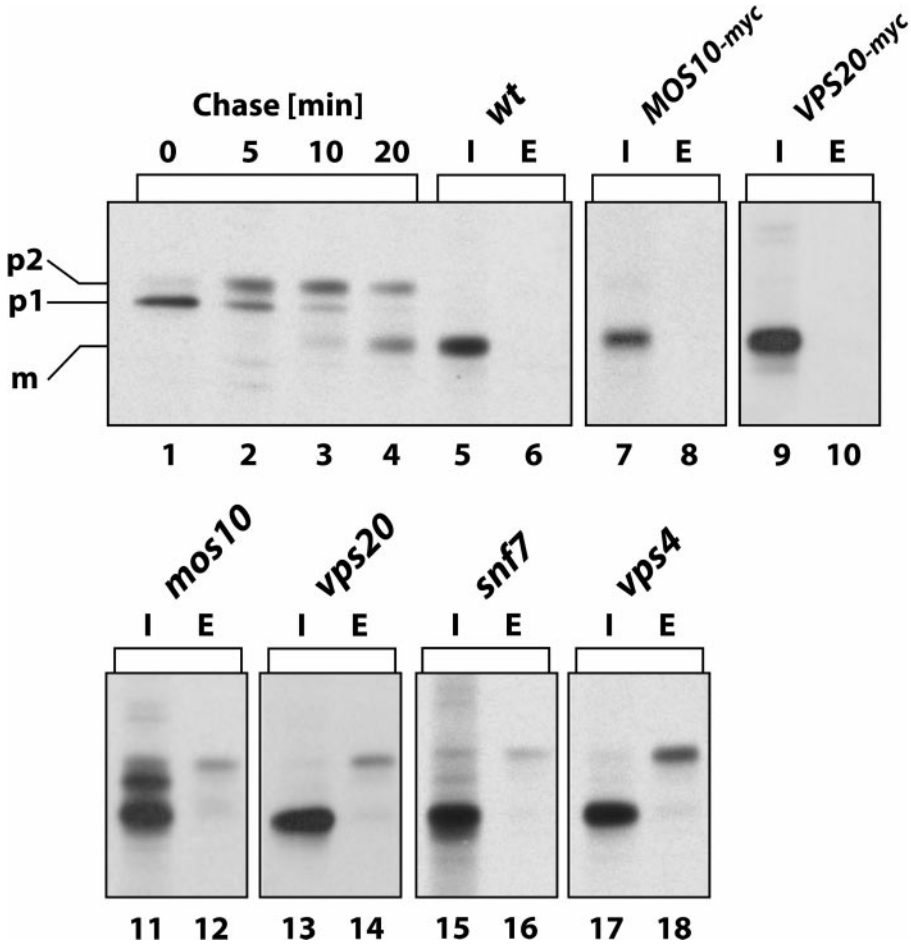

Figure 5. CPY sorting in deletion mutants. Cells were labeled for 10 min with [^{35}S] Trans label and chased with an excess of cold methionine and cysteine for 40 min. CPY was immunoprecipitated from spheroplast (internal, I) fractions and medium (external, E) fractions. The precipitated proteins were analyzed by SDS-PAGE and autoradiography. Lanes 5 and 6, JD52 (wild-type); lanes 7 and 8, RKY1452 (*MOS10-13myc*); lanes 9 and 10, RKY1633 (*VPS20-13myc*); lanes 11 and 12, RKY1509 (Δ*mos10*); lanes 13 and 14, RKY1590 (Δ*vps20*); lanes 15 and 16, RKY1510 (Δ*snf7*); and lanes 17 and 18, RKY1511 (Δ*vps4*). For comparison, CPY maturation was followed in the wild-type strain JD52 (lanes 1–4). Cells were briefly labeled (5 min) and chased for the time periods indicated. CPY was immunoprecipitated from whole cell extracts. The positions of the different CPY forms are indicated.

small ring-like structure next to the vacuole (Figure 7, C, E, and F). In some cells, a dot corresponding to this ring-like structure could be identified in the Nomarsky image. This ring-like structure most likely represents the "class E-compartment," corresponding to the late endosome in yeast (Raymond *et al.*, 1992). A similar FM4-64 staining pattern was observed with the Δ*mos10* mutant (Figure 7D), indicating that the same transport step is affected as in the other mutants.

Our previous experiments indicated that Ste6 is also transported along the endocytic pathway to the vacuole where it is degraded (Kölling and Hollenberg, 1994; Kölling and Losko, 1997). Ste6 can therefore be used as another endocytic marker to study the defect of the Δ*mos10* mutant. The distribution of c-myc-tagged Ste6, expressed from a multicopy plasmid, was examined by immunofluorescence staining. Overexpression had no effect on Ste6 half-life or distribution on sucrose gradients (our unpublished results). As reported

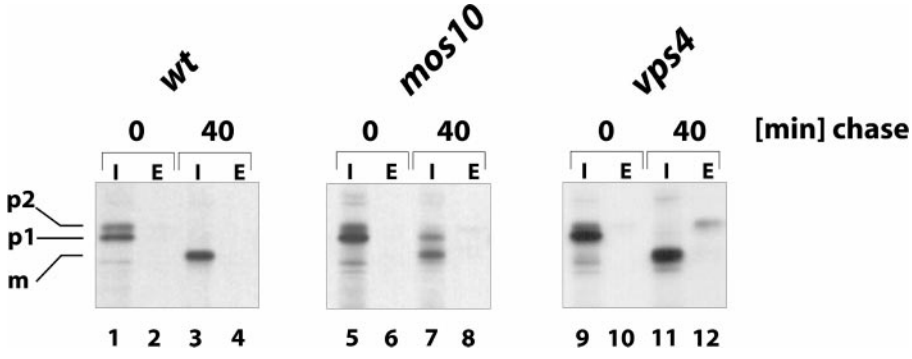

Figure 6. CPY sorting control. Cells were labeled for 5 min with [^{35}S] Trans label and chased with an excess of cold methionine and cysteine. CPY was immunoprecipitated from spheroplast (internal, I) fractions and medium (external, E) fractions at 0 and 40 min of chase. The precipitated proteins were analyzed by SDS-PAGE and autoradiography. Lanes 1–4, JD52 (wild-type); lanes 5–8, RKY1509 (Δ*mos10*); and lanes 9–12, RKY1511 (Δ*vps4*). The positions of the different CPY forms are indicated. The autoradiograms were scanned and the CPY signals were quantified with the program NIH Image 1.62.

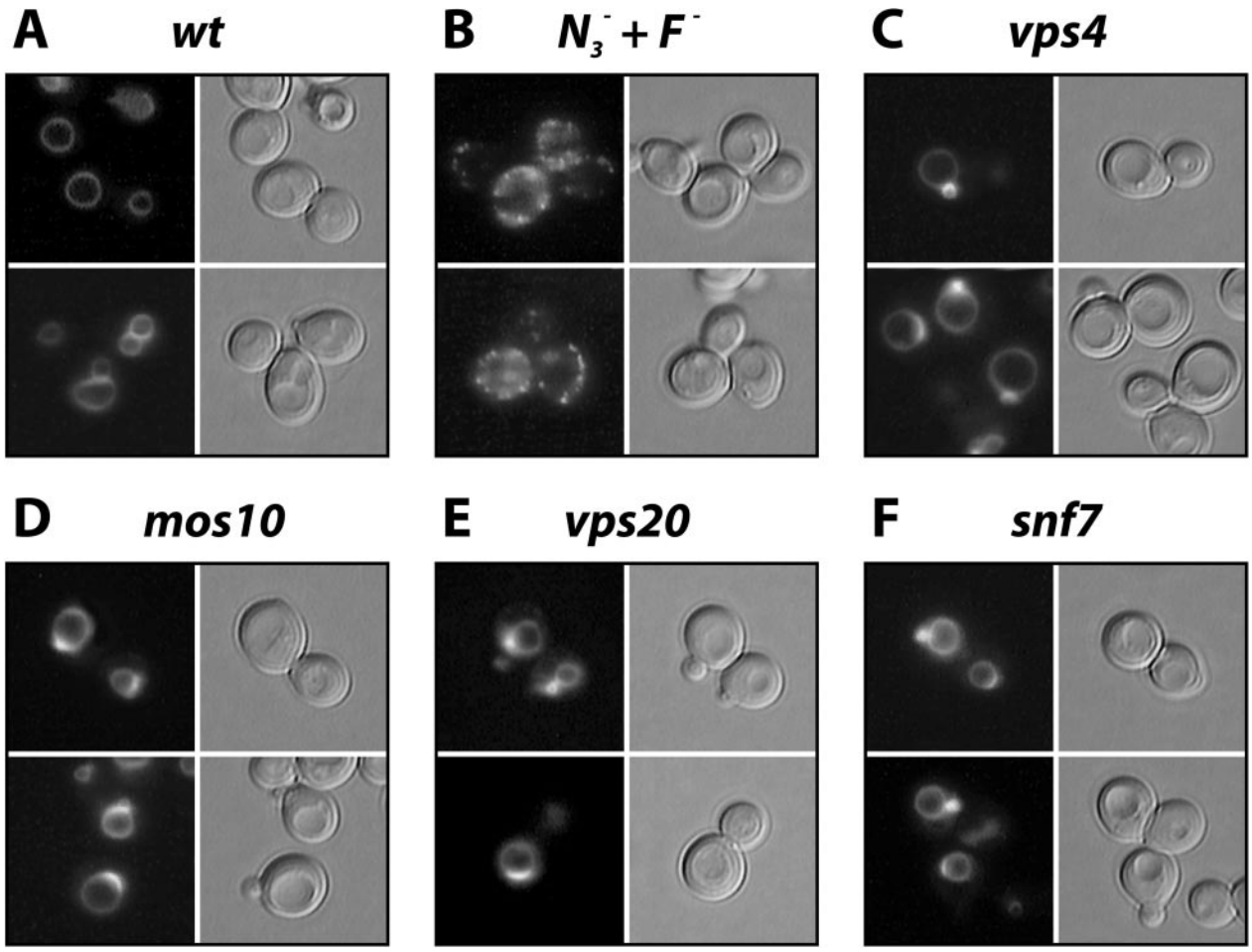

Figure 7. FM4-64 internalization in the deletion mutants. Cells were incubated for 30 min with the lipophilic dye FM4-64. After a 45–60-min chase period in medium without dye, FM4-64 fluorescence was examined. (A) JD52 (wild-type), (B) JD52 (10 mM NaN_3 + 10 mM NaF added together with FM4-64), (C) RKY1511 (Δ*vps4*), (D) RKY1509 (Δ*mos10*), (E) RKY1590 (Δ*vps20*), and (F) RKY1510 (Δ*snf7*). (Left) FM4-64 fluorescence. (Right) Nomarsky image.

previously (Kölling and Losko, 1997), a staining around the vacuole was observed in wild-type cells (Figure 8A). The vacuoles can be seen as light spots in the phase contrast image. The vacuole was also stained in the Δ*vps4*, Δ*mos10*, Δ*vps20*, and Δ*snf7* mutants (Figure 8, B–E). In addition, a brightly staining dot next to the vacuole (presumably the "class E dot") was observed in most of the cells. The staining was more intense in the mutant cells than in wild-type cells (signals adjusted to the same intensities in Figure 8). The Ste6 distribution was also examined using a Ste6-GFP fusion expressed from a multicopy plasmid. With the Ste6-GFP fusion, essentially the same fluorescence pattern was observed in the mutants as in the immunofluorescence experiment (our unpublished results). Accumulation of Ste6 in the prevacuolar compartment in a class E *vps* mutant has also been reported previously (Loayza and Michaelis, 1998).

Mos10 and Vps20 Are Associated with Membranes

Although the members of the Snf7 family are hydrophilic proteins, it has been demonstrated previously that a fraction of Snf7 is associated with membranes (Babst *et al.*, 1998). We were interested to see whether this is also true for the other two members of this protein family. For detection, the Snf7 family members were tagged with 13 c-myc tags at their C termini by integration of a PCR cassette behind the chromosomal open reading frames. CPY sorting was normal in the *MOS10-13myc* and *VPS20-13myc* strains (Figure 5), demonstrating that the tagged proteins are functional. The Snf7-13myc protein, however, turned out to be nonfunctional (our unpublished results) and was therefore excluded from further analysis. To obtain information about the intracellular localization of Mos10 and Vps20, differential centrifugation experiments were performed. Cell extracts prepared from the strains containing the tagged proteins were separated into P13-pellet and S13-supernatant by centrifugation for 10 min at 13,000 × *g*. The S13-supernatant was further centrifuged for 1 h at 100,000 × *g*, resulting in P100-pellet and S100-supernatant. Both Mos10 and Vps20 showed a very similar fractionation pattern (Figure 9). About half of the protein could be sedimented by centrifugation, indicat-

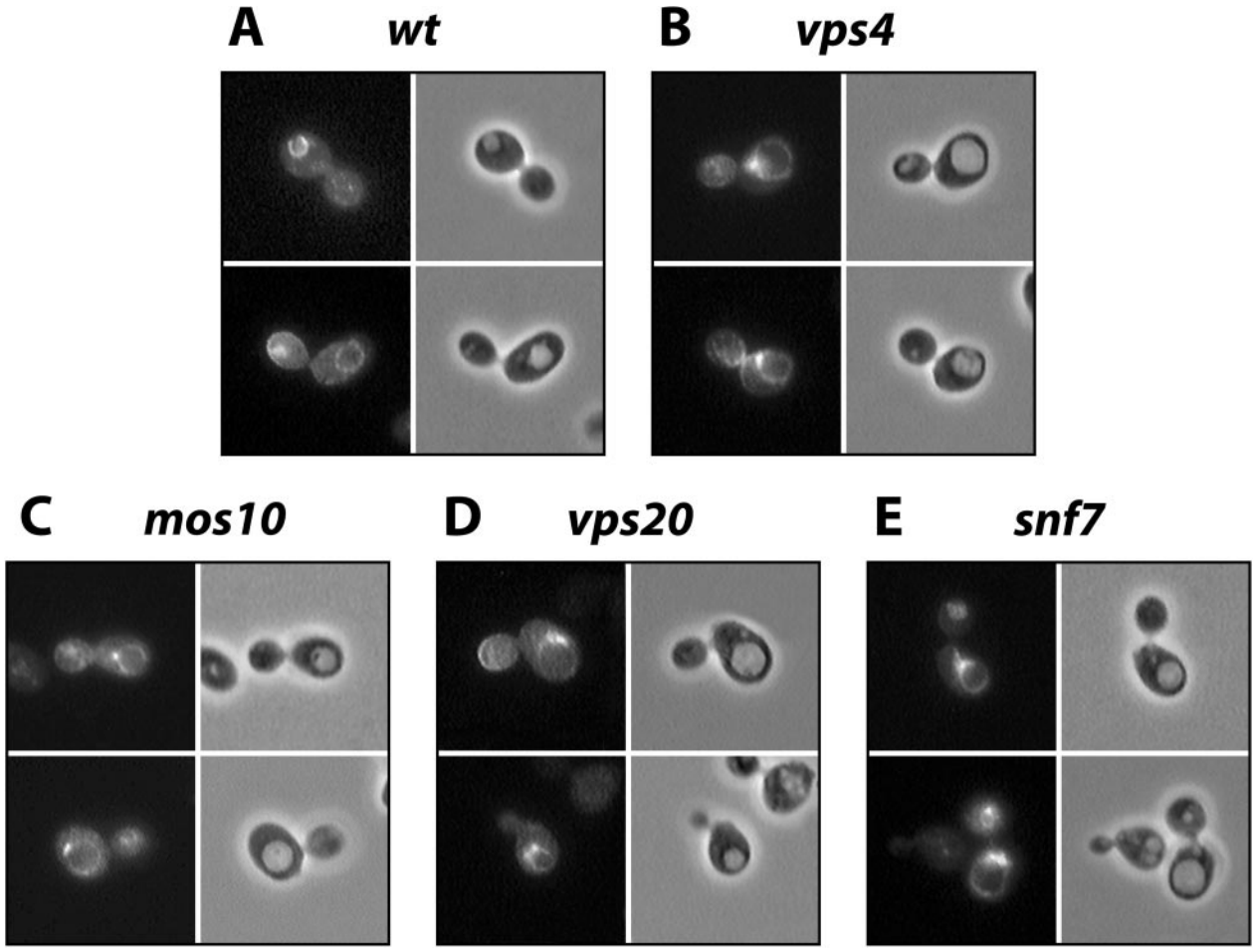

Figure 8. Localization of Ste6 by immunofluorescence. The c-myc-tagged Ste6 variant, encoded by pYKS2 (Kuchler *et al.*, 1993), was detected with anti-myc primary antibodies (9E10) and FITC-conjugated anti-mouse secondary antibodies in different strains. JD52 (wild-type) (A), RKY1511 (Δ*vps4*) (B), RKY1509 (Δ*mos10*) (C), RKY1590 (Δ*vps20*) (D), and RKY1510 (Δ*snf7*) (E). (Left) FITC-fluorescence. (Right) Phase contrast image.

ing that a large fraction is either part of a sedimentable protein complex or associated with membranes. Mos10 and Vps20 from the P13-pellet (~40% of total) could be solubilized by treatment with the detergent Triton X-100, demonstrating that this fraction is indeed membrane associated. The P100 fraction (~15% of total), however, proved to be detergent resistant.

For Snf7, a very similar fractionation pattern has been reported (Babst *et al.*, 1998). Membrane association of Snf7 appeared to be dependent on Vps4 activity. Under conditions where Vps4 was inactive, Snf7 was almost exclusively found in the P13 fraction, indicating that Vps4 could be required for dissociation of Snf7 from the membrane. To test whether Vps4 activity also affects membrane association of Mos10, lysates from a Δ*vps4 MOS10-13myc* strain were fractionated by centrifugation. A small but significant shift in the Mos10 distribution was observed. The amount of Mos10 in the P13-fraction was increased from 38% in wild type to 58% in the Δ*vps4* mutant (our unpublished results). Although the effects we observed were smaller than those previously reported for Snf7, these experiments suggest that Vps4 activity could also be important for membrane association of Mos10.

Mos10 Cofractionates with the Endosomal Marker Pep12

From differential centrifugation experiments, predictions about the intracellular localization of Mos10 can be made. In general, the P13 fraction primarily contains membranes derived from the vacuole, plasma membrane, endoplasmic reticulum, mitochondria, and nuclei, whereas the P100 fraction mainly contains Golgi membranes and transport vesicles. By Western blotting, the distribution of Mos10 between the different fractions was compared with the distribution of several marker proteins (Figure 10). As expected, the vacuolar marker protein alkaline phosphatase (ALP) and the plasma membrane marker Pma1 were mainly found in the P13 fraction. The endosomal marker Pep12 was equally distributed between P13 and P100, as reported previously (Becherer *et al.*, 1996). The Ste6 distribution very much resembled the Pep12 distribution, which further supports the

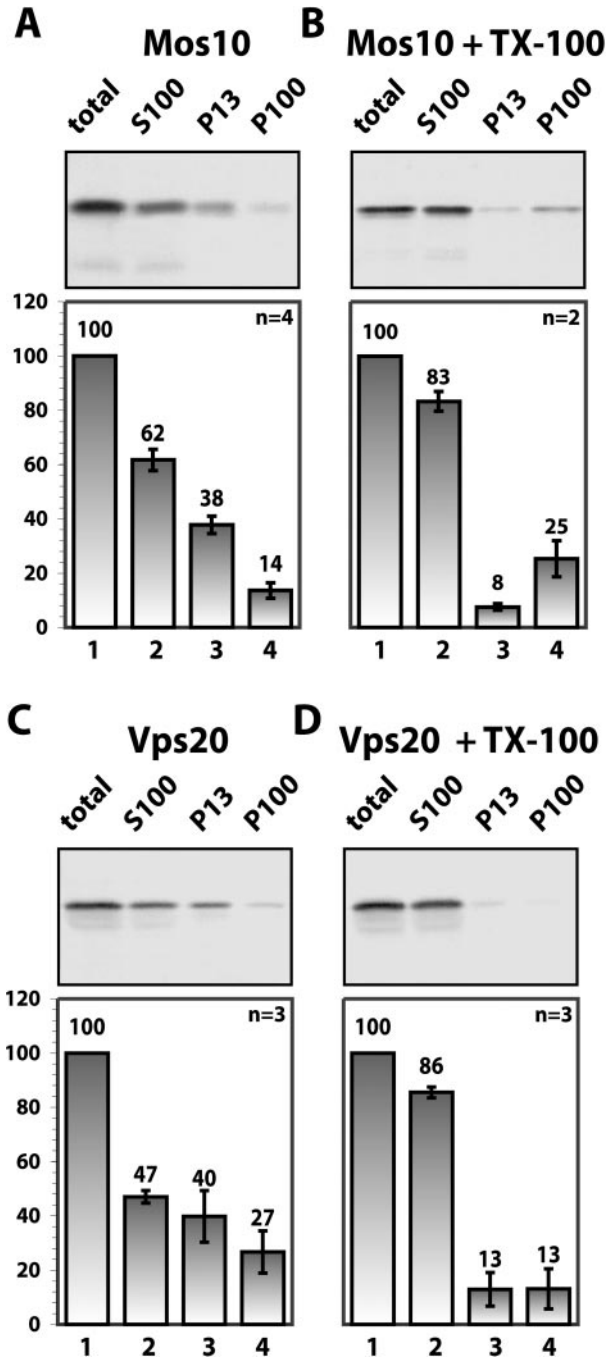

Figure 9. Fractionation of Mos10 and Vps20 by differential centrifugation. Cleared cell extracts were centrifuged at 13,000 × *g* for 10 min to pellet the P13 fraction. The supernatant was separated into a P100 pellet fraction and a S100 supernatant fraction by an additional centrifugation at 100,000 × *g* for 1 h. Equal portions of the fractions were analyzed by Western blotting with 9E10 antibodies directed against the 13myc-tagged proteins. RKY1452 (*MOS10-13myc*) (A), RKY1452 (*MOS10-13myc* + 2% Triton X-100) (B), RKY1633 (*VPS20-13myc*) (C), and RKY1633 (*VPS20-13myc* + 2% Triton X-100) (D). (Top) Western blots. (Bottom) Quantification of the Western blot signals. The signals of the total fractions were set to 100%. The average percentages (with SDs) of several experiments (n = 2–4) are shown.

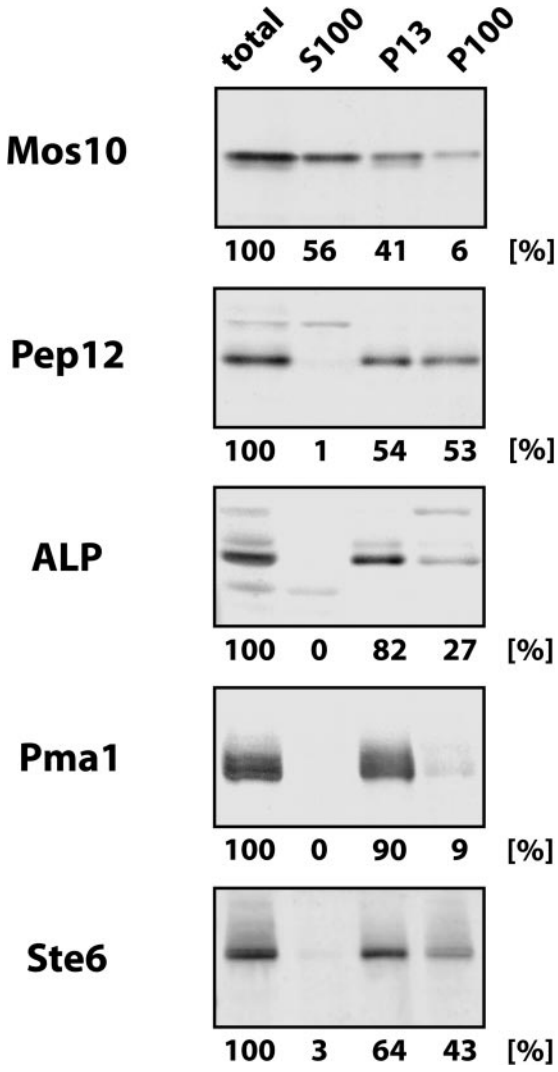

Figure 10. Fractionation of Mos10 in comparison to other cellular markers. Cell extracts of strain RKY1452 (*MOS10-13myc*) were fractionated by differential centrifugation as described in Figure 9. Equal portions of the fractions were analyzed for the presence of marker proteins by Western blotting with specific antibodies as indicated. A quantification of the signal intensities is given below the Western blot panels. The signals of the total fractions were set to 100%.

conclusions that Ste6 is localized to endosomal/vacuolar compartments. It is not clear whether the splitting of Pep12 between P13 and P100 reflects the localization to two different compartments with different sedimentation properties or whether Pep12 is localized to a single compartment that is only partially sedimented by the 13,000-g spin. As already described, sedimentable Mos10 was mainly found in the P13 pellet. From the Δ*mos10* phenotypes, it is unlikely that Mos10 acts at the endoplasmic reticulum or the plasma membrane. The most likely interpretation therefore is that Mos10 is localized to the vacuolar membrane (which sediments in the P13 pellet) or to a "Pep12-compartment" (i.e.,

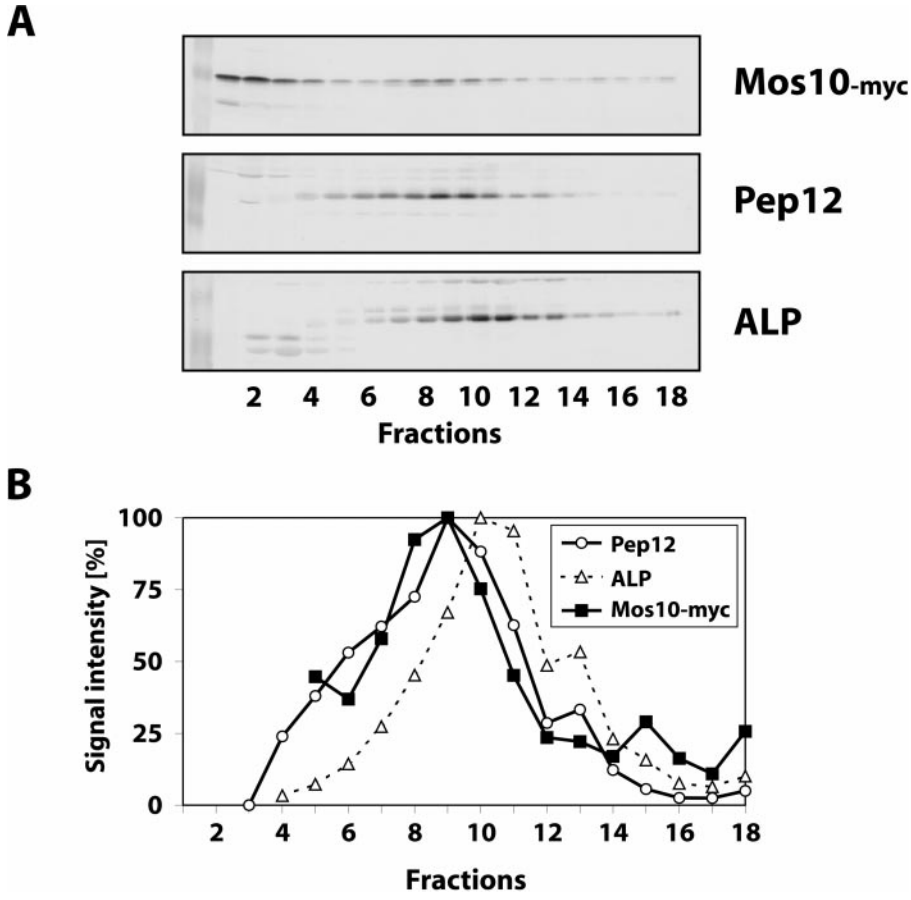

Figure 11. Fractionation of Mos10 by density gradient centrifugation. A whole cell extract of strain RKY1452 (*MOS10-13myc*) was fractionated on a sucrose density gradient (20–50% wt/wt sucrose, fraction 1: low-sucrose density). (A) Gradient fractions were analyzed for the presence of marker proteins by Western blotting with specific antibodies as indicated. (B) Densitometric quantification of the Western blot signals. The Western blots were scanned and the signal intensities were quantified with the program NIH Image 1.62. The strongest signals were set to 100%. Pep12 (○), ALP (△), and Mos10-[13myc (■).

endosomes) with sedimentation properties similar to the vacuolar membrane.

To gain additional information about the localization of Mos10, cell extracts were fractionated on sucrose density gradients. Fractions were collected from the gradients and analyzed for the presence of Mos10 and the marker proteins Pep12 and ALP by Western blotting (Figure 11). For Pep12, a broad peak with a shoulder toward the lower density fractions was observed, indicating that this peak is composed of two overlapping subfractions. The Pep12 peak was clearly separated from the ALP peak. For Mos10, we observed two peaks: one peak coincided with the soluble protein peak (fractions 1–4, not shown in Figure 11B) and one peak closely matched the higher density portion of the Pep12 peak (fractions 8–10). This is in line with the differential centrifugation experiments (Figure 9), which showed that about half of Mos10 is membrane associated, whereas the other half is soluble. This fractionation pattern of membrane-associated Mos10 suggests that Mos10 is localized to a Pep12-containing compartment, i.e., the prevacuolar compartment or late endosome, clearly distinct from the ALP-containing vacuolar membrane. The distribution of Vps20 on sucrose gradients could not be examined by this procedure, because membrane association of Vps20 was lost during gradient centrifugation.

DISCUSSION

We have identified several gene functions, which upon overproduction, interfere with the trafficking of the **a**-factor transporter Ste6 to the yeast vacuole. In addition to functions already known to be involved in vacuolar protein sorting (Snf7/Vps32, Vps4, and Vps35), we identified a new *VPS* function required for efficient sorting of CPY to the vacuole. Mutants defective for this *MOS10* gene accumulated the endocytic markers FM4-64 and Ste6 in a ring or dot-like structure next to the vacuole. This structure presumably represents an exaggerated form of the late endosome in yeast and is a hallmark of the so-called "class E *vps* mutants" (Raymond *et al.*, 1992). Accordingly, a very similar staining pattern was observed with Δ*snf7*, Δ*vps4*, and Δ*vps20*, which had been classified before as "class E *vps* mutants". *MOS10* does not correspond to any of the 13 "class E mutants" described so far (Emr, personal communication) and thus represents a new "class E function."

The Snf7 Protein Family

Mos10 turned out to be a member of a small family of coiled-coil–forming proteins. All three members of this protein family (Mos10, Snf7, and Vps20) appear to act at the level of the endosome. Upon inactivation, a pronounced "class E *vps* phenotype" was observed for each protein,

which suggests that all three proteins are essential for normal endosome-to-vacuole trafficking. The proteins could be part of a common structure, e.g., a coat complex, or could function independently at the same transport step.

The different growth phenotypes of the mutants, however, cannot be easily reconciled with a common function for the Snf7 family proteins. Mutants defective for Snf7 show a "sucrose nonfermenting phenotype," which results from a defect in invertase derepression under glucose-limiting conditions (Tu *et al.*, 1993). Apparently, glucose signaling is affected in this mutant. The "*snf*-phenotype" could be explained by altered turnover of a glucose sensor. Similarly, the ts-phenotype of Δ*snf7* could be explained by lack of removal of heat-damaged cell surface proteins. Although Δ*vps20* shows phenotypes very similar to Δ*snf7*, the Δ*mos10* mutant is neither temperature sensitive nor does it appear to have problems with invertase derepression. This suggests that the Snf7 family members display some sort of selectivity toward transported cargo proteins. The Snf7 family members could be specificity factors regulating docking and fusion of distinct transport vesicles with the endosome. Alternatively, the Snf7 family proteins could be involved in cargo selection in the multivesicular bodies pathway (Odorizzi *et al.*, 1998). The proteins could bind to certain subsets of cargo proteins maybe as part of a common coat structure. Although removal of one subunit would render the whole complex nonfunctional for endosome-to-vacuole transport, the remainining subunits could still sequester certain cargo proteins by binding to them thus explaining the different growth phenotypes of the mutants.

There is circumstantial evidence that Mos10 could be part of a larger protein complex. Because protein complexes are sensitive to changes in the stoichiometry of their components, our screen favors the isolation of functions that are part of protein complexes. Also, the existence of coiled-coil–forming regions in Mos10 strongly suggests that Mos10 forms homo or heteromeric complexes with other proteins. The Triton-resistant pool of Mos10 sedimenting in the 100,000-g pellet could correspond to such a larger Mos10-containing protein complex. However, so far we have not been able to demonstrate complex formation of Mos10 with other proteins. In native coimmunoprecipitation experiments, no specific bands could be coimmunoprecipitated with epitope-tagged Mos10 (our unpublished results).

Localization of Mos10

Our cell fractionation experiments are compatible with an endosomal localization of membrane-associated Mos10. On sucrose gradients, Mos10 cofractionated with the endosomal marker Pep12, which is found in a broad peak with a shoulder toward the lower density fractions. This profile suggests that the Pep12 peak consists of two overlapping subfractions derived from two distinct Pep12-containing membrane compartments. Mos10 cofractionated with the "heavy" portion of the Pep12 peak. Because Pep12 functions as an endosomal t-SNARE (Becherer *et al.*, 1996), the heavy Pep12 peak, which is also the main peak, most likely corresponds to endosomal membranes. It is clearly distinct from the peak of the vacuolar marker ALP. As a result of fusion between endosomes and the vacuole, Pep12 should also be incorporated into the vacuolar membrane. However, no cofractionation between Pep12 and the vacuolar membrane marker ALP was observed. This suggests that Pep12 is very efficiently retrieved from the vacuolar membrane and transported back to the endosome. The "light" Pep12 peak, i.e., the shoulder on the Pep12 profile, could thus correspond to transport vesicles engaged in retrieval of Pep12 from the vacuolar membrane.

ACKNOWLEDGMENTS

We thank Karl Köhrer, Hugh Pelham, and Dieter Wolf for the gift of CPY and Pep12 antibodies. We are also grateful to Jürgen Dohmen for stimulating discussions and to Cor Hollenberg for support. This work was supported by the Deutsche Forschungsgemeinschaft Grant Ko-963/2-3 and Ko-963/2-4 to R.K.

REFERENCES

Akada, R., Kallal, L., Johnson, D.I., and Kurjan, J. (1996). Genetic relationships between the G protein beta gamma complex, Ste5p, Ste20p and Cdc42p: investigation of effector roles in the yeast pheromone response pathway. Genetics *143*, 103–117.

Babst, M., Sato, T.K., Banta, L.M., and Emr, S.D. (1997). Endosomal transport function in yeast requires a novel AAA-type ATPase, Vps4p. EMBO J. *16*, 1820–1831.

Babst, M., Wendland, B., Estepa, E.J., and Emr, S.D. (1998). The Vps4p AAA ATPase regulates membrane association of a Vps protein complex required for normal endosome function. EMBO J. *17*, 2982–2993.

Bankaitis, V.A., Johnson, L.M., and Emr, S.D. (1986). Isolation of yeast mutants defective in protein targeting to the vacuole. Proc. Natl. Acad. Sci. USA *83*, 9075–9079.

Becherer, K.A., Rieder, S.E., Emr, S.D., and Jones, E.W. (1996). Novel syntaxin homologue, Pep12p, required for the sorting of lumenal hydrolases to the lysosome-like vacuole in yeast. Mol. Biol. Cell *7*, 579–594.

Erdman, S., Lin, L., Malczynski, M., and Snyder, M. (1998). Pheromone-regulated genes required for yeast mating differentiation. J. Cell Biol. *140*, 461–483.

Gietz, R.D., and Sugino, A. (1988). New yeast-*Escherichia coli* shuttle vectors constructed with in vitro mutagenized yeast genes lacking six-base pair restriction sites. Gene *74*, 527–534.

Jones, E.W. (1977). Proteinase mutants of *Saccharomyces cerevisiae*. Genetics *85*, 23–33.

Kölling, R., and Hollenberg, C.P. (1994). The ABC-transporter Ste6 accumulates in the plasma membrane in a ubiquitinated form in endocytosis mutants. EMBO J. *13*, 3261–3271.

Kölling, R., and Losko, S. (1997). The linker region of the ABC-transporter Ste6 mediates ubiquitination and fast turnover of the protein. EMBO J. *16*, 2251–2261.

Kuchler, K., Dohlman, H.G., and Thorner, J. (1993). The **a**-factor transporter (*STE6* gene product) and cell polarity in the yeast *Saccharomyces cerevisiae*. J. Cell Biol. *120*, 1203–1215.

Kuchler, K., Sterne, R.E., and Thorner, J. (1989). *Saccharomyces cerevisiae STE6* gene product: a novel pathway for protein export in eukaryotic cells. EMBO J. *8*, 3973–3984.

Loayza, D., and Michaelis, S. (1998). Role for the ubiquitin-proteasome system in the vacuolar degradation of Ste6p, the **a**-factor transporter in *Saccharomyces cerevisiae*. Mol. Cell. Biol. *18*, 779–789.

Longtine, M.S., McKenzie, A., 3rd, Demarini, D.J., Shah, N.G., Wach, A., Brachat, A., Philippsen, P., and Pringle, J.R. (1998). Additional modules for versatile and economical PCR-based gene deletion and modification in *Saccharomyces cerevisiae*. Yeast, *14*, 953–961.

Lupas, A. (1996). Prediction and analysis of coiled-coil structures. Methods Enzymol. *266*, 513–525.

McGrath, J.P., and Varshavsky, A. (1989). The yeast *STE6* gene encodes a homologue of the mammalian multidrug resistance P-glycoprotein. Nature *340*, 400–404.

Novick, P., Field, C., and Schekman, R. (1980). Identification of 23 complementation groups required for post-translational events in the yeast secretory pathway. Cell *21*, 205–215.

Odorizzi, G., Babst, M., and Emr, S.D. (1998). Fab1p PtdIns(3)P 5-kinase function essential for protein sorting in the multivesicular body. Cell *95*, 847–858.

Raymond, C.K., Howald, S.I., Vater, C.A., and Stevens, T.H. (1992). Morphological classification of the yeast vacuolar protein sorting mutants: evidence for a prevacuolar compartment in class E *vps* mutants. Mol. Biol. Cell *3*, 1389–1402.

Robinson, J.S., Klionsky, D.J., Banta, L.M., and Emr, S.D. (1988). Protein sorting in *Saccharomyces cerevisiae*: isolation of mutants defective in the delivery and processing of multiple vacuolar hydrolases. Mol. Cell. Biol. *8*, 4936–4948.

Rothman, J.H., and Stevens, T.H. (1986). Protein sorting in yeast: mutants defective in vacuole biogenesis mislocalize vacuolar proteins into the late secretory pathway. Cell *47*, 1041–1051.

Seaman, M.N., McCaffery, J.M., and Emr, S.D. (1998). A membrane coat complex essential for endosome-to-Golgi retrograde transport in yeast. J. Cell Biol. *142*, 665–681.

Tsien, R.Y. (1998). The green fluorescent protein. Annu. Rev. Biochem. *67*, 509–544.

Tu, J., Vallier, L.G., and Carlson, M. (1993). Molecular and genetic analysis of the *SNF7* gene in *Saccharomyces cerevisiae*. Genetics *135*, 17–23.

Vida, T.A., and Emr, S.D. (1995). A new vital stain for visualizing vacuolar membrane dynamics and endocytosis in yeast. J. Cell Biol. *128*, 779–792.

Wada, Y., Ohsumi, Y., and Anraku, Y. (1992). Genes for directing vacuolar morphogenesis in *Saccharomyces cerevisiae*. I. Isolation and characterization of two classes of *vam* mutants. J. Biol. Chem. *267*, 18665–18670.

Weisman, L.S., Emr, S.D., and Wickner, W.T. (1990). Mutants of *Saccharomyces cerevisiae* that block intervacuole vesicular traffic and vacuole division and segregation. Proc. Natl. Acad. Sci. USA, *87*, 1076–1080.

Zaal, K.J., Smith, C.L., Polishchuk, R.S., Altan, N., Cole, N.B., Ellenberg, J., Hirschberg, K., Presley, J.F., Roberts, T.H., Siggia, E., Phair, R.D., and Lippincott-Schwartz, J. (1999). Golgi membranes are absorbed into and reemerge from the ER during mitosis. Cell, *99*, 589–601.